Journal of Inflammation Research

Dovepress
Taylor & Francis Group

Open Access Full Text Article

ORIGINAL RESEARCH

Diagnostic and Prognostic Value of miR-574-3p in Acute Pancreatitis: Insights from Bioinformatics and in vitro Studies

Xueyan Wu, Danfeng Gong, Long Cheng, Jing Zhou

Department of Gastroenterology, Changde Hospital, Xiangya School of Medicine, Central South University (The First People's Hospital of Changde City), Changde, Hunan, People's Republic of China

Correspondence: Jing Zhou, Department of Gastroenterology, Changde Hospital, Xiangya School of Medicine, Central South University (The first People's Hospital of Changde City), 818 Renmin Road, Changde, Hunan, 415000, People's Republic of China, Email Zhoujingchde@163.com

Background: MicroRNA (miRNA) exists great potential as a biomarker for various diseases.

Purpose: This study aimed to explore the role and mechanism of miR-574-3p in acute pancreatitis (AP) to improve clinical management.

Patients and Methods: Clinical data from 241 AP patients (87 mild (MAP), 154 moderate-severe (M/SAP)) and 77 healthy controls were analyzed. Dysregulated miRNAs were screened via GEO, with expression levels quantified by qRT-PCR. The miR-574-3p value in AP was assessed via ROC curves, correlation analysis, and multivariate logistic regression. Caerulein-induced HPDE6-C7 cell models were employed to evaluate the effects of miR-574-3p on proliferation, oxidative stress, and inflammation. Luciferase assays confirmed miR-574-3p/EGFR interaction.

Results: MiR-574-3p was downregulated in AP and lower in M/SAP than in MAP patients, demonstrating its diagnostic utility. MiR-574-3p was negatively associated with AP severity as evidenced by its correlation with the scoring systems, including Ranson, APACHE II, and SOFA, and served as a risk factor for poor prognosis of M/SAP. In vitro, miR-574-3p overexpression promoted cell proliferation, reduced oxidative stress (decreased MDA, increased SOD), and suppressed inflammation (IL-6, IL-1β, TNF-α) in caerulein-stimulated HPDE6-C7 injury model. EGFR was identified as a downstream gene of miR-574-3p, and its upregulation reversed the protective effects of miR-574-3p.

Conclusion: MiR-574-3p, associating with AP severity, served as a diagnostic biomarker for AP and M/SAP. MiR-574-3p was identified as a risk factor for the poor prognosis of M/SAP and involved in pancreatic cell injury through regulating EGFR. This work highlighted the clinical potential of miR-574-3p for AP diagnosis, prognosis and therapeutic strategies.

Keywords: acute pancreatitis, miR-574-3p, biomarker, EGFR, mechanism

Introduction

The pancreas, a vital organ located behind the stomach, plays a crucial role in digestion and blood sugar regulation by producing digestive enzymes and hormones.[1] When these enzymes become activated within the pancreas instead of in the small intestine, they start digesting the pancreatic tissue itself, leading to inflammation and potential damage.[2] Acute pancreatitis (AP), an acute inflammatory disorder of the pancreas characterized by varying severity from self-limiting episodes to systemic multiorgan failure, represents a critical gastrointestinal emergency with substantial global health implications.[3] Epidemiological data indicate a global AP incidence of 34 cases per 100,000 population and high mortality rate of approximate 40%, with rising trends attributed to obesity, alcohol consumption, and biliary disorders.[4–6] The clinical presentation of AP varies widely, making early diagnosis and disease severity assessment challenging. Current diagnostic methods, such as serum amylase and lipase levels, while widely used, have limitations in sensitivity and specificity as they are normal in patients with alcoholic or hypertriglyceridaemia pancreatitis, often leading to delayed or incorrect diagnosis.[7] Furthermore, these markers do not always correlate with the severity of the disease or predict its progression.[8] Therefore,

https://doi.org/10.2147/JIR.S542184
Received: 9 June 2025
Accepted: 18 November 2025
Published: 17 January 2026

there is an urgent need to identify novel biomarkers that can accurately diagnose AP, predict disease severity, and monitor treatment response. The discovery of such biomarkers would significantly enhance the ability to manage AP clinically, potentially reducing the morbidity and mortality associated with AP.

MicroRNAs (miRNAs) are small non-coding RNAs (18–25 nt) regulating gene expression through post-transcriptional silencing, playing pivotal roles in cell functions and multiple biological processes.[9] Dysregulated miRNA expression has also been reported to be linked to AP progression, with specific miRNAs emerging as potential biomarkers and therapeutic targets. For instance, serum miR-216a, miR-216b, miR-217, miR-92b, miR-375 and miR-148a were upregulated in AP and could serve as novel biomarkers for AP.[10] In addition, upregulated miR-126-5p expression in mild AP (MAP) and severe AP (SAP) patients is associated with AP severity and serum cytokine levels, indicating miR-126-5p might be a potential biomarker for AP severity.[11] In mechanistic studies, miR-325-3p overexpression could attenuate the injury of pancreatic acinar cells by targeting PIPK3 in AP.[12] Downregulation of miR-132-3p in AP is reported to be involved in pancreatic ductal epithelial cell injury by regulating TRAF3 expression, thereby affecting the activation of the NF-κB signaling pathway.[13] Furthermore, miRNA-based therapies, such as antisense oligonucleotides targeting pro-inflammatory miRNAs, show promise in preclinical models.[14] Further exploration of miRNA regulatory networks and cross-talk with their downstream gene may unlock novel mechanistic insights, accelerating clinical translation to improve outcomes in AP patients.

MiR-574-3p has been increasingly recognized for its involvement in various pathological conditions, including osteosarcoma, myocarditis, and osteoarthritis.[15–17] Notably, accumulating evidence suggests its critical role in regulating inflammatory processes, with studies demonstrating that downregulation of miR-574-3p promotes oxygen-glucose deprivation-induced microglial inflammation and oxidative stress.[18] Additionally, miR-574-3p overexpression has been shown to suppress glucose-glucose-induced pancreatic β-cell dysfunction through modulation of PRMT1 expression.[19] These findings might highlight the potential involvement of miR-574-3p in AP pathogenesis.

Based on the emerging evidence implicating dysregulated miRNAs in disease progression, there might be specific miRNA that is aberrantly expressed in AP and functionally contribute to disease progression through modulation of critical cellular functions. This study aimed to identify specific AP-associated miRNA by screening datasets from the GEO database, followed by clinical validation of candidate miRNAs in patient cohorts to to identify the potential dysregulated miRNA-miR-574-3p, and assess its diagnostic potential. Furthermore, elucidating the mechanistic roles of miR-574-3p through in vitro functional experiments may deepen the understanding of miR-574-3p-mediated regulatory mechanism in pancreatic injury and provide a theoretical foundation for developing miR-574-3p-based interventions and therapeutical potential to improve clinical management of AP.

Materials and Methods

Selection of Clinical Subjects

Sample size was calculated using G*Power 3.1 software with an a priori *t*-test design. Parameters included an effect size of 0.5, α error probability of 0.05, and statistical power of 0.8, resulting in a required sample size of 64 subjects per group. This study consecutively enrolled 241 AP patients diagnosed at Changde Hospital, Xiangya School of Medicine, Central South University (The first people's hospital of Changde city) between Jan 1st 2022 and Dec 31st 2024, alongside 77 age and sex matched healthy controls (HC group) undergoing routine physical examinations during the same periods, with the sample size reached an effect size of 0.5, α error probability of 0.05, and statistical power of 0.97 through the post hoc *t* test. AP diagnosis was confirmed by revised Atlanta criteria,[20] integrating clinical symptoms (abdominal pain, serum amylase/lipase levels exceeding more than three times the upper limit), and imaging evidence (contrast-enhanced ultrasonography). Disease severity was classified as mild, moderate, and severe based on the 2012 Atlanta classification: mild AP featured no organ failure and local/systemic complications, moderately severe AP included transient organ failure (< 48 hours) and/or local or systemic complications without persistent organ failure, and severe AP was defined as persistent organ failure (> 48 hours). Final AP cohorts comprised 87 mild AP (MAP group) and 154 moderate to severe AP (M/SAP group) subjects. Ethical approval (No.2021–253-01) was obtained from the Ethics Committee of Changde Hospital, Xiangya School of Medicine, Central South University (The first people's hospital of Changde city). All subjects had signed the informed consent.

Exclusion criteria of AP: 1) chronic pancreatitis or acute onset of chronic pancreatitis, 2) malignancy-induced pancreatitis, 3) pregnancy, 4) other severe infections, tumors, chronic heart, brain, liver and kidney diseases, blood system diseases and immune diseases, 5) AP caused by iatrogenic reasons such as endoscopic retrograde cholangiopancreatography or other surgeries, 6) incomplete clinical data. Healthy controls were excluded for any pancreatic disorders, systemic inflammatory diseases, or recent infections Supplemantary Figure 1.

Cells

HPDE6-C7 (human pancreatic duct epithelial cells) cell line was obtained from the American Type Culture Collection (ATCC, US).

Bioinformatics Analysis

Using "pancreatitis" and "miR" as the keywords to search the proper databases. Differentially expressed miRNAs in pancreatitis were screened from the public datasets GSE123377, GSE128425, and GSE173514, which were obtained from the Gene Expression Omnibus (GEO) database (https://www.ncbi.nlm.nih.gov/geo/). Overlapping miRNAs across the three datasets, specified by p values of less than 0.05, were visualized via a Venn diagram. Shared miRNAs further underwent expression level validation.

Potential targets of miR-574-3p were predicted independently using TargetScanHuman (https://www.targetscan.org/vert_80/) and Starbase (https://rnasysu.com/encori/), followed by the intersection of predicted gene lists via Venn analysis. Functional annotation of overlapping genes was performed using the DAVID platform (https://davidbioinformatics.nih.gov/tools.jsp) for Gene Ontology (biological processes) and KEGG pathway enrichment.

Clinical Information of All Subjects and Sample Processing

Baseline demographic and clinical parameters, including age, gender, body mass index (BMI), hypertension (HTN), and diabetes mellitus (DM) history, were systematically recorded for all enrolled participants. The scoring system, including Ranson, APACHE II, and SOFA, was calculated by at least three specialists.

Fasting venous blood samples were collected in the morning using standardized protocols and analyzed immediately for biochemical indices such as white blood cell count (WBC), triglycerides (TG), and C-reactive protein (CRP) using an automated clinical chemistry analyzer (Roche Cobas 8000, Switzerland).

For subsequent gene expression analysis, whole blood samples were centrifuged at 3700 rpm for 10 minutes to collect serum, which was stored at −80 °C until further processing.

For M/SAP subjects, the poor prognosis, including disease progression and death, was recorded accordingly before they were discharged from the hospital.

Cell Culture, Stimulation, and Transfection

Human pancreatic ductal epithelial HPDE6-C7 cells (ATCC, US) were maintained in Ham's F12 medium (Gibco, US) supplemented with 10% fetal bovine serum (FBS, Gibco, US) and 1% penicillin-streptomycin (Sigma-Aldrich, Germany) at 37 °C in a humidified 5% CO_2 incubator. The HPDE6-C7 cells were passaged when the cell confluency reached 70–80%, and then used for the further experiment at the passage of 4–6.

To establish the HPDE6-C7 injury model, the cells were treated with 10 nM caerulein (MedChemExpress, USA) for 12 hours under standard culture conditions, as previously validated.[13]

Transfection of HPDE6-C7 cells was performed using Lipofectamine 3000 (Thermo Fisher Scientific, US) according to the manufacturer's guidelines. For miRNA modulation, cells were transfected with 50 nM miR-574-3p mimic or 100 nM miR-574-3p inhibitor (Ribobio, China), with mimic and inhibitor NC serving as respective negative controls. EGFR overexpression was achieved via transfection of 2 μg/mL recombinant pcDNA3.1-EGFR plasmid (oe EGFR, Thermo Fisher Scientific, US), while the empty pcDNA3.1 vector (Thermo Fisher Scientific, US) served as the overexpression control (oe NC). Post-transfection, cells were maintained in standard conditions (37 °C, 5% CO_2) for 48 hours prior to collection.

Quantitative Real-Time Polymerase Chain Reaction

Total RNA was isolated from serum and cell lysates using TRIzol reagent (Thermo Fisher Scientific, US) following the manufacturer's protocols. RNA concentration and purity were quantified via a NanoDrop Lite spectrophotometer (Thermo Fisher Scientific, US), with samples demonstrating A260/280 ratios between 1.8–2.0 selected for downstream analysis. Reverse transcription was performed with 1 μg RNA using SuperScript™ III First-Strand Synthesis System (Invitrogen, US). Quantitative PCR amplification was conducted using PowerTrack™ SYBR Green Master Mix (Applied Biosystems, US) on a 7500 Real-Time PCR System (Applied Biosystems, US), with thermal cycling conditions: 95 °C for 10 minutes (initial denaturation), followed by 40 cycles of 95 °C for 15 seconds and 60 °C for 1 minutes. MiRNAs expression was normalized to cel-miR-39 spike-in control, while EGFR levels were standardized to GAPDH. Relative quantification was calculated using the $2^{-\Delta\Delta Ct}$ method.

Cell Viability Assessment

Following transfection or pharmacological stimulation, viable cells were quantified and plated in 96-well culture plates (Corning, US) at a density of 1×10^3 cells/well. Cells were maintained under standard culture conditions (37 °C, 5% CO_2) for longitudinal viability assessment at 0, 24, 48, and 72 hours timepoints. At each interval, 10 μL of CCK-8 reagent (Dojindo Molecular Technologies, Japan) was added to each well, followed by a 2-hour incubation. Absorbance at 450 nm was quantified using a BioTek Synergy H1 Hybrid Reader (Agilent Technologies, US) after gentle plate agitation to ensure homogeneous colorimetric distribution. Background absorbance from reagent-only wells was subtracted prior to data normalization.

Cell Oxidative Stress and Inflammation Evaluation

Oxidative stress biomarkers were quantified through malondialdehyde (MDA) and superoxide dismutase (SOD) assays. Post-treatment cells were rinsed with ice-cold PBS and lysed in RIPA buffer (Beyotime, China) containing protease inhibitors. Lysates were centrifuged at 12000 rpm for 15 min under the temperature of 4 °C, and supernatants were collected. MDA levels (Beyotime, China) were quantified using a thiobarbituric acid (TBA) assay: supernatants were mixed with TBA, heated at 95°C for one hour, cooled, and absorbance measured at 532 nm. SOD activity (Beyotime, China) was analyzed via a WST-8-based kit. Lysates were incubated with the reaction mix for 20 minutes at 37 °C, and absorbance was read at 450 nm.

Inflammatory cytokines ELISA kits were employed for the evaluation of the inflammatory response of the cells. Cell culture supernatants were centrifuged at 1000 rpm for 10 minutes to remove debris. IL-6, IL-1β, and TNF-α levels were quantified using human ELISA kits (Abcam, England) according to the manufacturer's protocol. Absorbance at 450 nm was measured after TMB substrate development (30 minutes incubation in the dark).

Investigation on the Interaction Between miR-574-3p and EGFR

The binding sites of miR-574-3p on the EGFR sequence were predicted by the TargetScanHuman database, and their regulatory relationship was validated through dual-luciferase reporter assay. The EGFR 3'-UTR sequences containing predicted miR-574-3p binding sites were cloned into pmirGLO vectors (Promega, US), serving as the EGFR wild type (EGFR-WT) and the mutant type (EGFR-MUT) was conducted by mutating at the binding sites. The EGFR WT or MUT reporter plasmids were co-transfected with 50 nM miR-574-3p mimics, 100 nM miR-574-3p inhibitors, or negative control (NC) using Lipofectamine 3000 in HPDE6-C7 cells, respectively. After 48 hours of incubation (37 °C, 5% CO_2), cells were lysed, and firefly/Renilla luciferase activities were measured sequentially using the Dual-Luciferase Reporter Assay System (Promega, US).

Statistical Analysis

All statistical analyses were conducted using IBM SPSS Statistics 26.0 and GraphPad Prism 9.0. Continuous variables with normal distribution were compared between two groups using an unpaired Student's *t*-test, while categorical variables were analyzed via a chi-square test. Multi-group comparisons employed one-way ANOVA with Tukey's post-

hoc testing. Diagnostic performance was evaluated through receiver operating characteristic (ROC) curve analysis. Correlation between miR-574-3p expression and AP severity was analyzed by Spearman correlation analysis. Prognostic risk factors for M/SAP were identified using multivariable logistic regression analysis. In vitro experiments included three independent biological replicates with technical triplicates. Data were expressed as mean ± standard deviation (SD). Statistical significance was defined as $p < 0.05$.

Results

Clinical Information Comparison

The clinical characteristics of the study cohorts were summarized in Table 1. Demographic and baseline metabolic parameters, including age, gender distribution, BMI, HTN, and DM prevalence, showed no statistically significant differences across HC, MAP, and M/SAP groups ($p > 0.05$). Comparative analysis revealed significantly elevated WBC counts, TG levels, and CRP concentrations in both MAP and M/SAP cohorts relative to HC ($p < 0.001$). Notably, the M/SAP group demonstrated progressive increases in inflammatory markers and organ dysfunction scores compared to MAP patients, with significantly higher WBC, CRP, Ranson, APACHE II, and SOFA scores ($p < 0.001$). However, TG levels showed no significant intergroup difference between MAP and M/SAP cohorts ($p = 0.445$).

The Expression of miRNAs and the ROC Curve

Four overlapping miRNAs in the three databases (GSE123377, GSE128425, and GSE173514) were revealed by the Venn diagram, namely miR-3613-3p, miR-548a-3p, miR-502-3p, and miR-574-3p (Figure 1a). There was no expression difference between the HC and AP groups in miR-3613-3p ($p = 0.483$, Figure 1b), miR-548a-3p ($p = 0.483$, Figure 1c), and miR-502-3p ($p = 0.169$, Figure 1d) expression ($p > 0.05$). The serum miR-574-3p expression was

Table 1 Clinical Information of the Subjects

Index		HC (n = 77)	MAP (n = 87)	M/SAP (n = 154)	*p* value		
					p1	p2	p3
Age (year)		50.18 ± 7.64	50.64 ± 8.67	51.89 ± 9.92	0.943	0.370	0.563
Gender	Male	41	55	89	0.196	0.512	0.409
	Female	36	32	65			
BMI (kg/m^2)		23.16 ± 1.09	23.19 ± 1.05	22.96 ± 1.05	0.975	0.392	0.243
HTN	Y	11	16	33	0.479	0.193	0.574
	N	66	71	121			
DM	Y	10	19	29	0.138	0.264	0.574
	N	67	68	125			
WBC ($\times 10^9/L$)		6.60 ± 1.41	17.29 ± 1.76	18.26 ± 2.44	<0.001	<0.001	0.001
TG (mmol/L)		1.12 ± 0.12	1.75 ± 0.22	1.79 ± 0.26	<0.001	<0.001	0.445
CRP (mg/L)		3.72 ± 0.57	29.63 ± 7.70	64.88 ± 29.71	<0.001	<0.001	<0.001
Ranson Score		–	1.97 ± 0.20	3.30 ± 0.79	–	–	<0.001
APACHE II		–	9.05 ± 2.18	17.46 ± 6.01	–	–	<0.001
SOFA Score		–	3.70 ± 1.61	8.34 ± 2.93	–	–	<0.001

Abbreviations: HC, healthy control; MAP, mild acute pancreatitis; M/SAP, moderate to severe acute pancreatitis; BMI, body mass index; HTN, hypertension; DM, diabetes mellitus; WBC, white blood cells; TG, triglycerides; CRP, C-reactive protein; APACHE II, Acute Physiology and Chronic Health Evaluation; SOFA, Sequential Organ Failure Assessment; *p*1: HC vs MAP, *p*2: HC vs M/SAP, *p*3: MAP vs M/SAP.

https://doi.org/10.2147/JIR.S542184

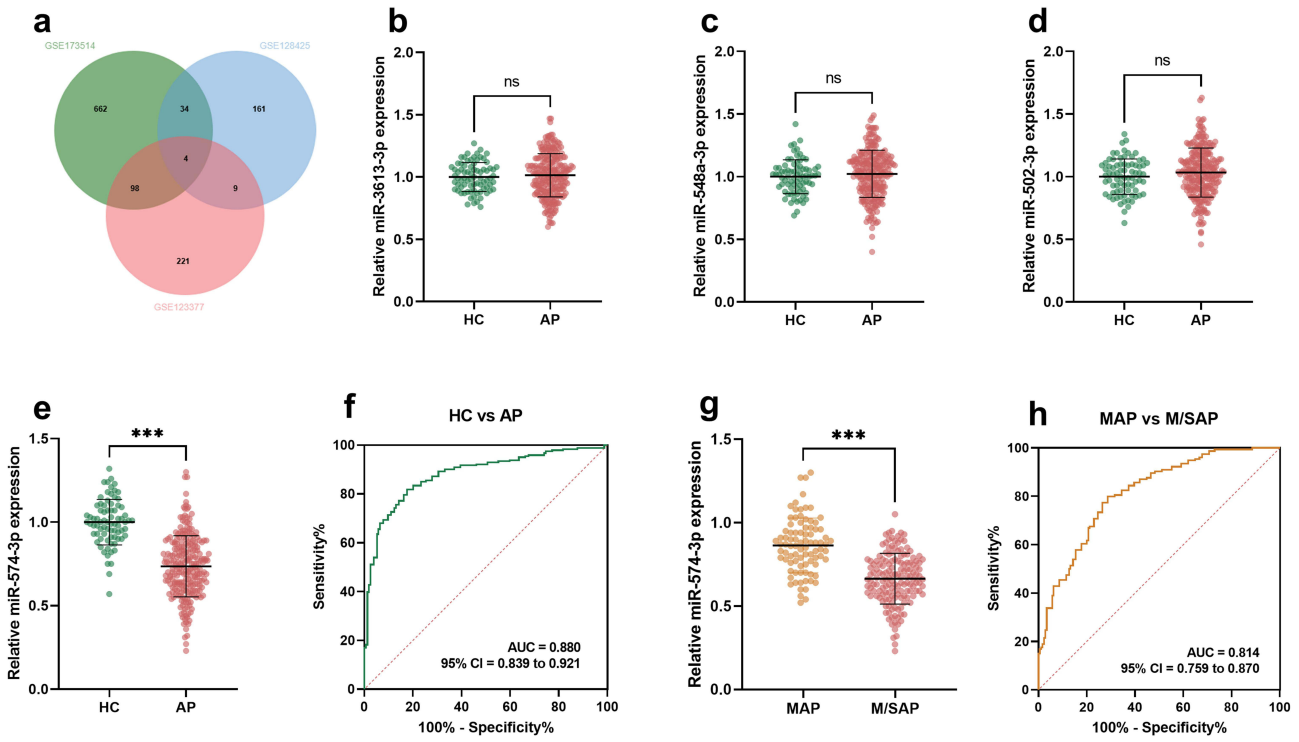

Figure 1 MiRNAs expression in the serum of subjects and the ROC curve. (**a**) Venn diagram of the overlapped miRNAs in GSE173514, GSE128425, and GSE123377 datasets. (**b–e**) The miRNA expression levels: (**b**) MiR-3613-3p; (**c**) MiR-548a-3p; (**d**) MiR-502-3p; (**e**) MiR-574-3p. (**f**) The ROC curve of miR-574-3p in distinguishing AP from healthy individuals. (**g**) The miR-574-3p expression was lower in M/SAP than that in MAP. (**h**) The ROC curve of miR-574-3p in differentiating M/SAP from AP subjects. ns: no significance, ***$p < 0.001$.

downregulated in comparison to the healthy individuals ($p < 0.001$, Figure 1e) and showed significant diagnostic value in AP (Figure 1f) with the AUC value of 0.880 (sensitivity: 81.74%, specificity: 81.82%, 95% CI: 0.839–0.921).

The miR-574-3p expression in the subjects with M/SAP was further decreased than that of the subjects with MAP ($p < 0.001$, Figure 1g). The downregulated miR-574-3p expression in M/SAP also showed the diagnostic value by distinguishing M/SAP from MAP with an AUC of 0.814, sensitivity of 79.87%, and specificity of 70.11% (95% CI: 0.759–0.870, Figure 1h).

Association Between miR-574-3p Expression and AP Severity

MiR-574-3p expression levels showed a significant clinical association with AP severity (Figure 2). Serum miR-574-3p was observed to be negatively correlated with the Ranson (r = −0.739, $p < 0.001$, Figure 2a), APACHE II (r = −0.648, $p <$

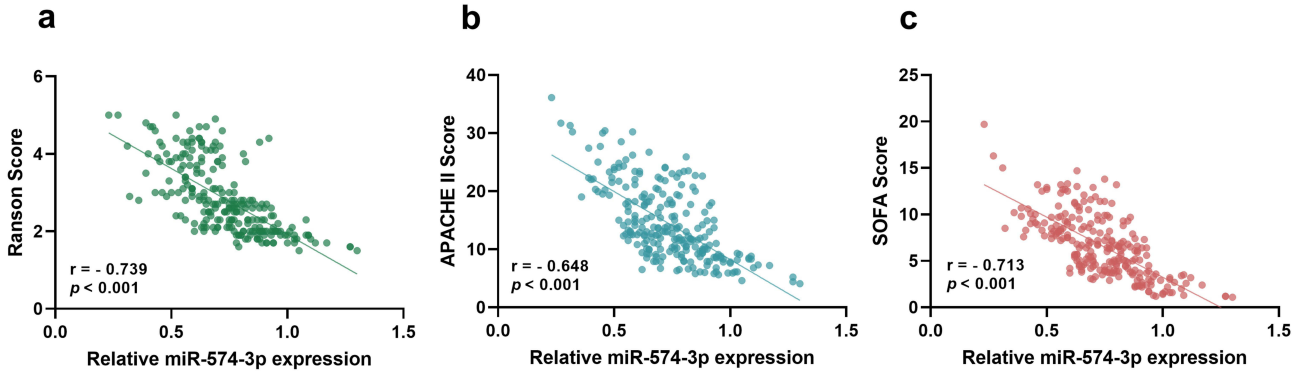

Figure 2 The association between miR-574-3p expression and AP severity. (**a**) The miR-574-3p expression was negatively correlated with the Ranson score. (**b**) The miR-574-3p expression was negatively correlated with the APACHE II score. (**c**) The miR-574-3p expression was negatively correlated with the SOFA score.

https://doi.org/10.2147/JIR.S542184

0.001, Figure 2b), and SOFA (r = −0.713, $p < 0.001$, Figure 2c) scores. These findings suggested an inverse association between serum miR-574-3p levels and disease progression in AP patients.

Risk Factors for the Poor Prognosis of M/SAP

Multivariate logistic regression analysis (Table 2) identified miR-574-3p as a risk factor for poor prognosis of M/SAP with the OR value of 0.349 (95% CI: 0.147–0.831, $p = 0.017$). In addition, the scoring system of Ranson (OR = 2.469, 95% CI: 1.073–5.684), APACHE II (OR = 2.274, 95% CI: 1.010–5.116), and SOFA (OR = 2.396, 95% CI: 1.054–5.448) could also serve as the risk factors for predicting poor prognosis of M/SAP.

The Effect of miR-574-3p on Caerulein-Induced HPDE6-C7 Injury

In vitro experimental analysis revealed significant suppression of miR-574-3p expression in HPDE6-C7 cells following caerulein induction ($p < 0.001$, Figure 3a). Caerulein treatment also inhibited HPDE6-C7 cell proliferation ($p < 0.001$, Figure 3b) while concurrently exacerbating oxidative stress and inflammatory responses, as evidenced by elevated MDA levels ($p < 0.001$, Figure 3c), reduced SOD activity ($p < 0.001$, Figure 3d), and increased secretion of pro-inflammatory cytokines ($p < 0.001$) including IL-6 (Figure 3e), IL-1β (Figure 3f), and TNF-α (Figure 3g). Strikingly, miR-574-3p overexpression in this cell injury model restored its expression levels ($p = 0.007$) and markedly attenuated caerulein-induced HPDE6-C7 injury by enhancing cellular proliferation ($p = 0.002$), suppressing MDA accumulation ($p < 0.001$), restoring SOD activity ($p < 0.001$), and significantly downregulating inflammatory cytokine production ($p < 0.001$).

Bioinformatics Analysis of miR-574-3p Downstream Genes and the Interaction Validation Between miR-574-3p and EGFR

The downstream genes of miR-574-3p were predicted through integrated analysis using TargetScan and Starbase databases, with 100 overlapping candidate genes identified at their intersection (Figure 4a). Subsequent functional

Table 2 Multivariate Logistic Regression Analysis on the Risk Factors of AP Poor Prognosis

Variable	OR	95% CI		*p* value
		Lower Limit	Upper Limit	
miR-574-3p	0.349	0.147	0.831	0.017
Age	1.558	0.684	3.551	0.291
BMI	1.499	0.648	3.470	0.344
Gender	1.466	0.658	3.265	0.350
HTN	1.714	0.582	5.046	0.328
DM	1.370	0.496	3.782	0.543
WBC	1.815	0.761	4.331	0.179
TG	1.347	0.597	3.038	0.473
CRP	1.493	0.642	3.476	0.352
Ranson Score	2.469	1.073	5.684	0.034
APACHE II	2.274	1.010	5.116	0.047
SOFA Score	2.396	1.054	5.448	0.037

Abbreviations: OR, odds ratio; CI, confidence interval; BMI, body mass index; HTN, hypertension; DM, diabetes mellitus; WBC, white blood cells; TG, diabetes mellitus; CRP, C-reactive protein; APACHE II, Acute Physiology and Chronic Health Evaluation; SOFA, Sequential Organ Failure Assessment.

https://doi.org/10.2147/JIR.S542184

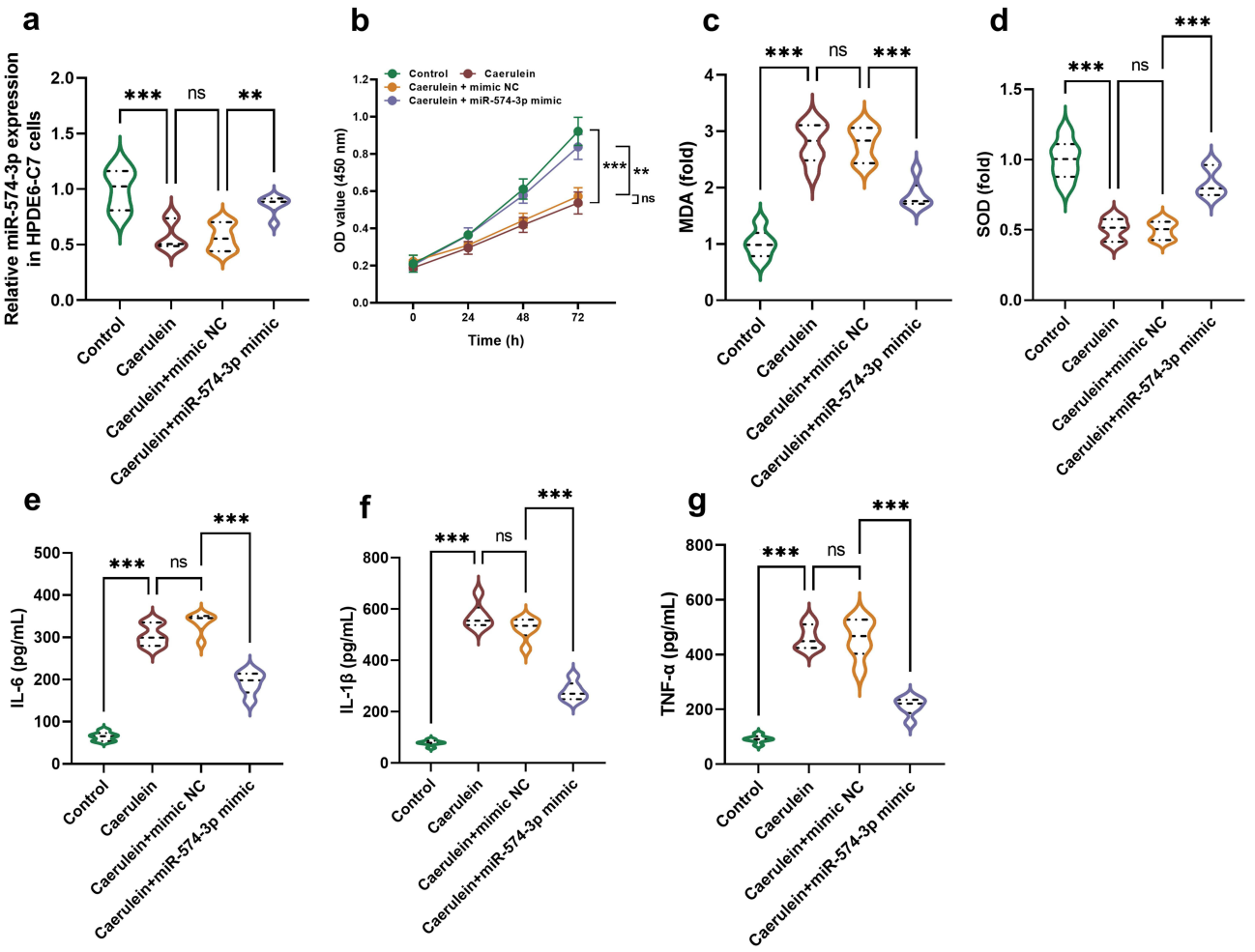

Figure 3 The effect of miR-574-3p in caerulein-stimulated HPDE6-C7 injury. (**a**) MiR-574-3p overexpression restored the downregulated miR-574-3p expression. (**b**) MiR-574-3p overexpression improved cell proliferation. (**c** and **d**) MiR-574-3p overexpression suppressed the oxidative stress: (**c**) MDA level; (**d**) SOD activity. (**e–g**) MiR-574-3p overexpression inhibited the inflammatory response: (**e**) IL-6 level; (**f**) IL-1β; (**g**) TNF-α. ns: no significance, $^{**}p < 0.01$, $^{***}p < 0.001$.

enrichment analysis of these targets revealed 26 significant Gene Ontology (GO) annotations and 10 KEGG pathways. Biological process (BP) annotations demonstrated predominant enrichment in transcriptional regulation mechanisms, particularly negative regulation of RNA polymerase II-mediated transcription, alongside protein ubiquitination and vesicular transport processes (Figure 4b). Cellular component (CC) analysis highlighted subcellular localization in cytosol, nucleus, and cytoplasmic compartments (Figure 4c). Molecular function (MF) characterization identified protein binding as the primary activity, supplemented by metal ion coordination capabilities (Figure 4d). Pathway analysis (Figure 4e) uncovered critical involvement in oncogenic pathways, human cytomegalovirus infection responses, and JAK-STAT signaling cascade regulation. The genes enriched in each term were revealed in Supplementary Table 1.

EGFR was selected for further analysis as it was identified to be involved in various pathways regulated by miR-574-3p and was reported to be dysregulated in AP previously. The binding sites between miR-574-3p and EGFR were predicted by the TargetScanHuman online database (Figure 5a). The regulatory relationship between miR-574-3p and EGFR was further validated by the dual-luciferase reporter assay. The luciferase activity of EGFR-WT (Figure 5b) could be suppressed by the miR-574-3p overexpression ($p = 0.006$), while inhibition of miR-574-3p expression could lead to the elevated luciferase activity of EGFR-WT ($p = 0.004$). No significant difference was observed in luciferase activity among the EGFR-MUT groups ($p > 0.05$, Figure 5c). Additionally, caerulein-treated HPDE6-C7 cells exhibited marked EGFR upregulation ($p < 0.001$), which could be attenuated by miR-574-3p overexpression ($p < 0.001$) but exacerbated through miR-574-3p knockdown ($p = 0.004$) in the HPDE6-C7 injury model (Figure 5d).

https://doi.org/10.2147/JIR.S542184

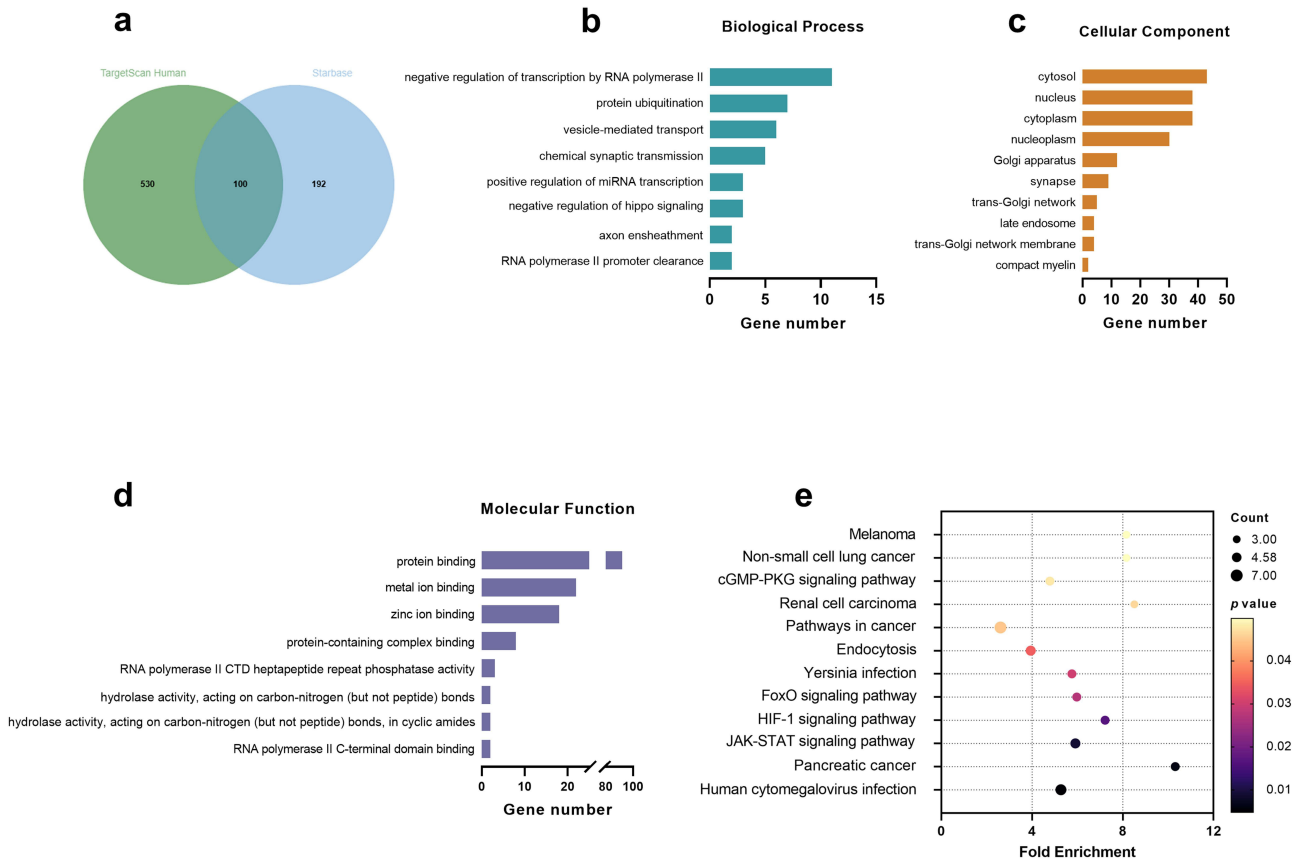

Figure 4 Bioinformatics analysis of miR-574-3p downstream genes and their functions. (**a**) Venn diagram of miR-574-3p downstream genes. (**b–d**) GO analysis: (**b**) Biological process; (**c**) Cellular component; (**d**) Molecular functions. (**e**) KEGG analysis on the signaling pathways.

The Effect of miR-574-3p/EGFR Axis on the HPDE6-C7 Injury Model

The cytoprotective effects of miR-574-3p overexpression against caerulein-induced injury in HPDE6-C7 cells were counteracted by EGFR overexpression. This could be observed through the suppressed cellular proliferation ($p = 0.027$, Figure 6a), exacerbated oxidative damage characterized by elevated MDA levels ($p = 0.006$, Figure 6b) and diminished SOD activity ($p < 0.001$, Figure 6c), and anabatic pro-inflammatory response with increased secretion of IL-6 ($p < 0.001$, Figure 6d), IL-1β ($p = 0.026$, Figure 6e), and TNF-α ($p < 0.001$, Figure 6f).

Discussion

MiRNAs have revolutionized our understanding of disease mechanisms across diverse pathologies, encompassing cancer, cardiovascular disorders, and inflammatory conditions.[21–23] Their ability to fine-tune cellular processes, including proliferation, apoptosis, and immune modulation through their extensive network of target gene interactions, positions miRNAs as master regulators of pathophysiological cascades.[9] Notably, miRNAs exhibit unparalleled advantages as biomarkers: exceptional stability in biofluids, resistance to enzymatic degradation, and dynamic expression patterns reflecting real-time pathological alterations.[24] Furthermore, miRNA benefits from well-established detection platforms (qRT-PCR) and comprehensive databases, ensuring methodological reproducibility and cross-species applicability.[25] Circulating miRNAs, detectable through minimally invasive methods, demonstrate tissue-specific signatures and superior sensitivity compared to conventional protein biomarkers. Therefore, identifying dysregulated miRNAs in AP may provide novel insights into AP clinical management.

To identify potential miRNA biomarkers in AP, this study enrolled a total of 241 AP patients and 77 demographically matched healthy individuals. Distinct systemic inflammatory and metabolic alterations in AP patients were revealed in this work, as evidenced by significantly elevated WBC count, TG, and CRP levels. These biomarkers collectively reflect

https://doi.org/10.2147/JIR.S542184

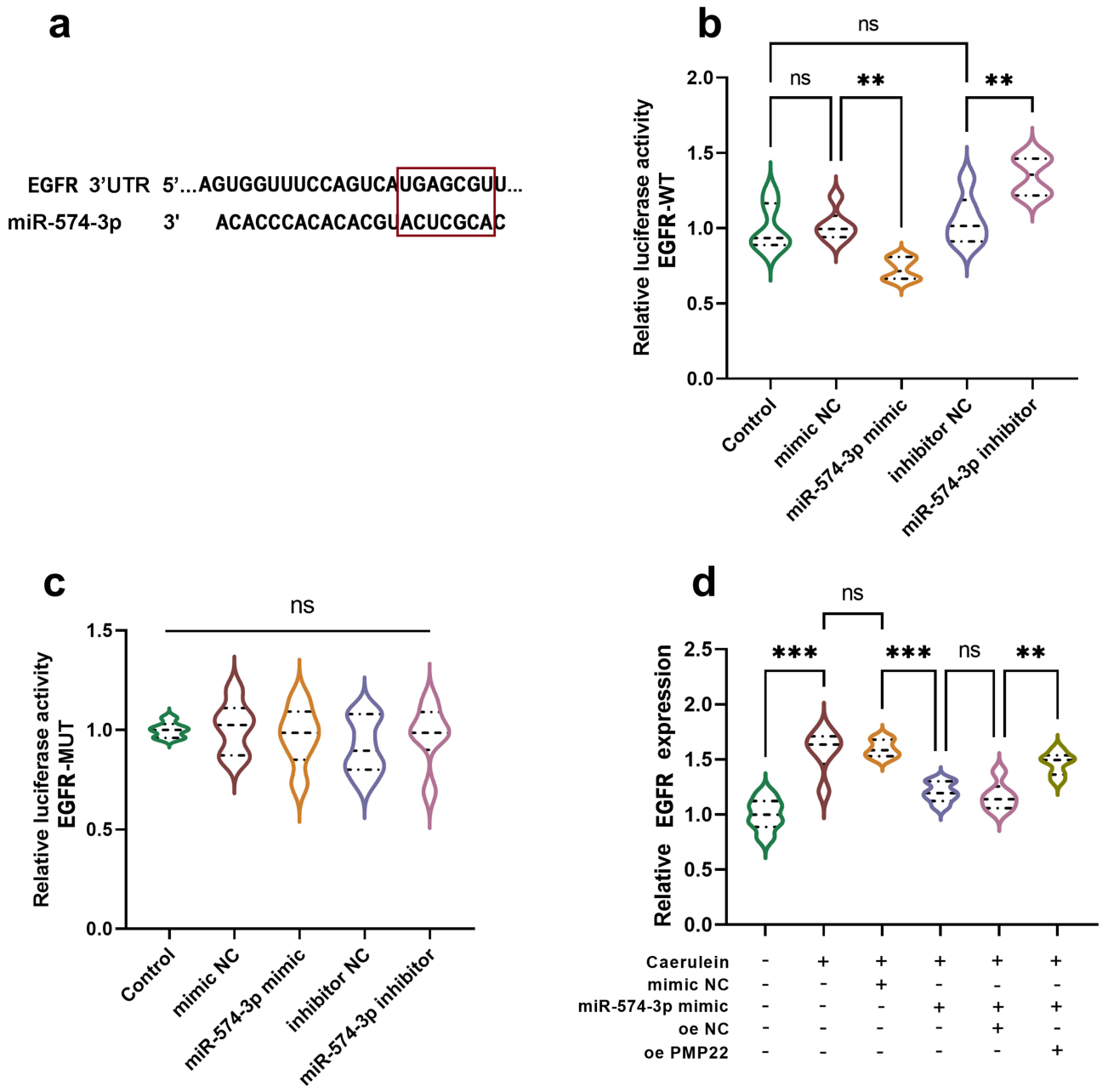

Figure 5 Interaction validation between miR-574-3p and EGFR. (**a**) The binding sites of miR-574-3p in EGFR which was circled by the red rectangular box were predicted by TargetScanHuman. (**b-c**) Dual-luciferase reporter assay: (**b**) MiR-574-3p overexpression suppressed the luciferase activity of EGFR-WT, which could be further improved by miR-574-3p downregulation; (**c**) No significant difference in luciferase activity could be observed in the EGFR-MUT group after miR-574-3p overexpression or knockdown. (**d**) Upregulated EGFR expression was observed in caerulein-induced HPDE6-C7 cell injury, and this upregulation of EGFR could be attenuated by miR-574-3p overexpression and further facilitated by EGFR overexpression. ns: no significance, $^{**}p < 0.01$, $^{***}p < 0.001$.

the hyperinflammatory state and metabolic dysregulation characteristic of AP pathogenesis.[26] The WBC level underscores neutrophil-driven tissue injury and systemic immune activation, while elevated TG level highlights lipid metabolic disturbances often implicated in AP etiology.[27,28] CRP, a hepatocyte-derived acute-phase reactant, is synthesized in response to IL-6 during tissue injury and could reflect the severity of the inflammatory cascade triggered by pancreatic damage in AP.[29,30] Notably, further elevations in WBC and CRP in M/SAP patients compared to mild cases emphasized the more severe inflammatory state of M/SAP patients who may be complicated by organ failure. According to the GEO database screening, four dysregulated miRNAs were identified, among which serum miR-574-3p exhibited obvious downregulation in AP and could serve as a diagnostic biomarker for both AP and M/SAP according to the ROC curve.

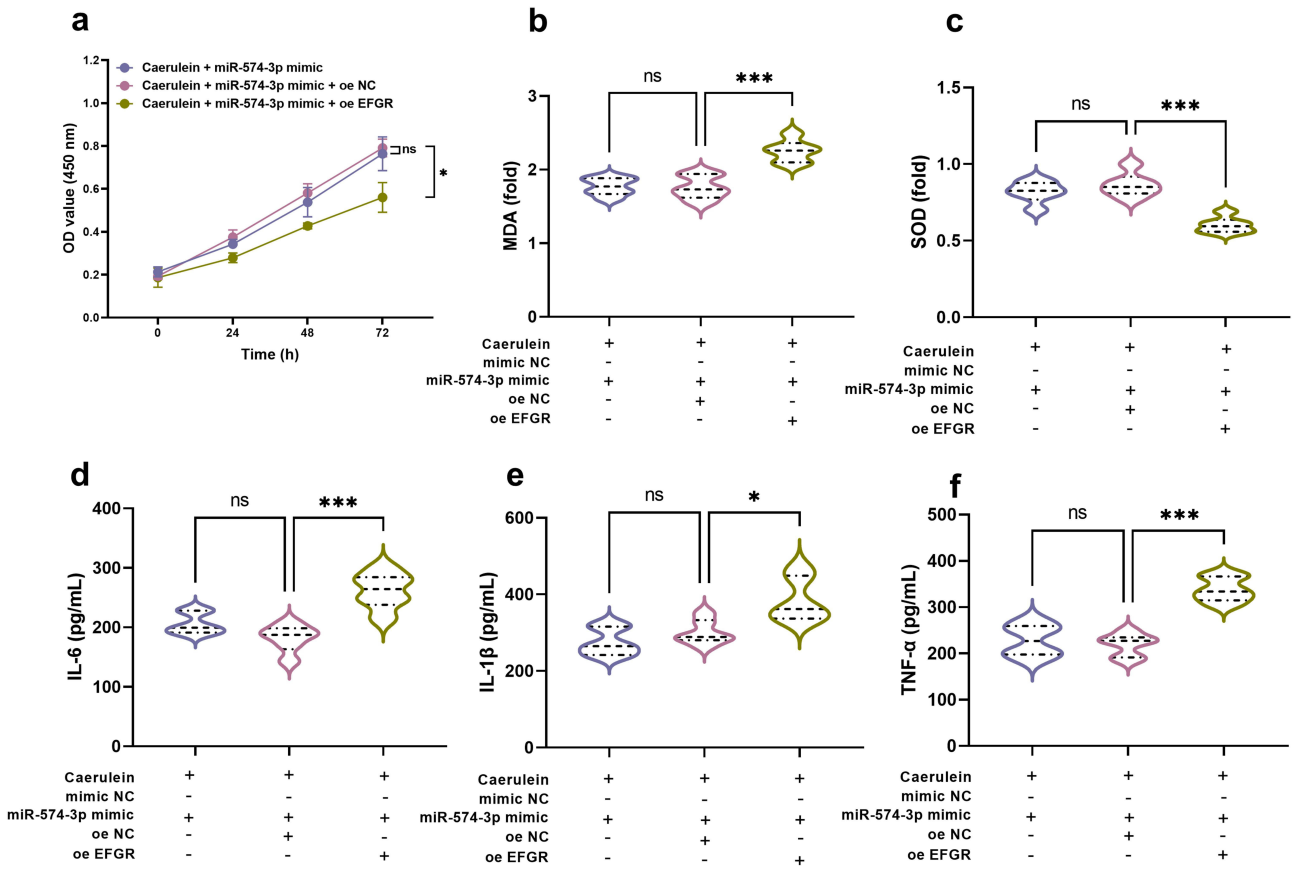

Figure 6 The effect of miR-574-3p/EGFR axis in caerulein-induced HPDE6-C7 cell injury. (**a**) The EGFR overexpression reversed the improved cell proliferation. (**b-c**) The EGFR overexpression promoted the suppressed oxidative stress: (**b**) MDA level; (c) SOD activity. (**d-f**) The EGFR overexpression increased the inhibited inflammation: (**d**) IL-6 level; (**e**) IL-1β; (**f**) TNF-α. ns: no significance, *$p < 0.05$, ***$p < 0.001$.

The correlation between miR-574-3p and AP may also be reflected by a previous study that showed miR-574-3p was decreased in high glucose-induced pancreatic islet β cell injury, as this injury could also be stimulated by AP progression.[19,31] In this work, the association between miR-574-3p and AP was further validated through the correlation analysis on miR-574-3p with the scoring system including Ranson, APACHE II, and SOFA. The scoring systems of Ranson, APACHE II, and SOFA are often used as the severity evaluation method in AP, and increased Ranson, APACHE II, and SOFA scores were observed in the M/SAP patients concerning the MAP patients, which was aligned with a prior study.[32] The negative relationship between miR-574-3p expression and these scoring systems reflected downregulated miR-574-3p closely associated with AP severity. Multivariate logistic regression confirmed miR-574-3p, Ranson, APACHE II, and SOFA scores as risk factors for poor prognosis of M/SAP, advocating their integration into early intervention protocols to mitigate complications or even death of AP patients. Given the comprehensive findings presented above, miR-574-3p demonstrated remarkable diagnostic efficacy for AP with distinct expression patterns. Its ability to accurately stratify disease severity, coupled with its prognostic predictive capabilities, positioned miR-574-3p as a promising dual-functional biomarker that could significantly enhance AP management strategies through integrated diagnostic and prognostic applications.

The injury of pancreatic ductal epithelial cells (PDECs) plays a pivotal role in the pathogenesis of AP. As the first-line barrier, PDEC damage triggers premature intracellular trypsinogen activation, initiating autodigestion and inflammatory cascades. To elucidate the mechanistic role of miR-574-3p in AP, a caerulein-induced pancreatic ductal epithelial cell (HPDE6-C7) injury was employed in this study. Caerulein, a cholecystokinin analog, induces PDEC injury through hyperstimulation of CCK receptors, leading to intracellular calcium overload and premature trypsinogen activation. This

https://doi.org/10.2147/JIR.S542184

will increase reactive oxygen species (ROS) production and trigger inflammatory cytokine release, collectively exacerbating ductal barrier dysfunction and AP progression.[33] Caerulein is a well-established in vitro system to recapitulate AP-related ductal damage, which has been validated by prior studies.[13,34] In this model, miR-574-3p downregulation coincided with suppressed cell proliferation, exacerbated oxidative stress (elevated MDA and reduced SOD), and amplified secretion of pro-inflammatory cytokines (IL-6, IL-1β, TNF-α), collectively mirroring AP-associated epithelial dysfunction. Notably, miR-574-3p overexpression attenuated caerulein-induced injury by restoring cell proliferation, mitigating oxidative damage, and dampening inflammatory responses, underscoring its cytoprotective function. Bioinformatic analysis via TargetScanHuman and Starbase identified potential downstream genes of miR-574-3p and revealed that these genes were related to biological processes, including transcriptional repression, protein ubiquitination, and JAK-STAT signaling pathways, which were implicated in AP pathogenesis.[35–37] Among the candidates, EGFR was validated as a target of miR-574-3p via dual-luciferase assays. EGFR, previously reported to be upregulated in the AP rat model,[38] was also confirmed to be upregulated in caerulein-treated HPDE6-C7 cells. The association between EGFR and the oxidative inflammatory cascade reaction was reported previously in the formulation of double cortistatin-like kinase 1 positive pancreatic stem cells.[39] In this work, the relation between EGFR, oxidative stress, and inflammation was also validated. Crucially, EGFR overexpression reversed the protective effects of miR-574-3p, suggesting that miR-574-3p alleviated ductal injury by suppressing EGFR-driven pathways. These findings positioned miR-574-3p as a critical regulator of oxidative-inflammatory cascades in HPDE6-C7 injury by regulating EGFR expression. By controlling this critical signaling pathway, miR-574-3p might be presented as promising therapeutic potential for specifically targeting epithelial damage during AP progression, offering novel mechanistic insights and innovative approaches for clinical AP management strategies.

While this study provided valuable insights into the role of miR-574-3p and associated indicators in AP, several limitations should be acknowledged. First, the relatively small sample size might limit the statistical power and generalizability of our findings, necessitating validation in larger, multi-center cohorts. Second, the exclusive reliance on in vitro HPDE6-C7 cell models, despite their physiological relevance, lacked corroboration from in vivo animal experiments, which are critical for assessing systemic effects and translational potential. Third, although bioinformatic predictions and luciferase assays identified EGFR as a downstream gene of miR-574-3p, comprehensive validation of the implicated signaling pathways (JAK-STAT, oxidative stress cascades) through mechanistic studies remained pending. Future studies should integrate in vivo AP models (caerulein- or L-arginine-induced AP in rodents) and multi-omics approaches to elucidate the broader regulatory network of miR-574-3p. Addressing these gaps would strengthen the clinical applicability of our findings.

Conclusion

This study revealed significant downregulation of miR-574-3p in AP and established its potential as a diagnostic biomarker for both AP and M/SAP patients. Importantly, miR-574-3p expression levels showed strong correlation with AP severity and served as a risk factor for poor M/SAP prognosis. In vitro investigations suggested that miR-574-3p downregulation might involved in AP progression by suppressing cellular viability while simultaneously promoting oxidative stress and inflammatory responses in HPDE6-C7 cell injury through regulating the EGFR expression. These findings of this study might provide a novel potential biomarker for the clinical management of AP and offer a new theoretical foundation for the development of clinical treatment strategies for this disease.

Disclosure

The author(s) report no conflicts of interest in this work.

References

1. Oh S, Kim YJ, Park YT, Kim KG. automatic pancreatic cyst lesion segmentation on eus images using a deep-learning approach. *Sensors*. 2021;22(1):245. doi:10.3390/s22010245
2. Aune D, Mahamat-Saleh Y, Norat T, Riboli E. High body mass index and central adiposity is associated with increased risk of acute pancreatitis: a meta-analysis. *Dig Dis Sci*. 2021;66(4):1249–1267. doi:10.1007/s10620-020-06275-6

3. Mahat RK, Rathore V, Saxena R. Association of Triglyceride-Glucose (TyG) index with severe acute pancreatitis: a systematic review and meta-analysis. *Cureus*. 2025;17(5):e83795. doi:10.7759/cureus.83795
4. Luo T, Tang Y, Xie W, et al. Cerium-based nanoplatform for severe acute pancreatitis: achieving enhanced anti-inflammatory effects through calcium homeostasis restoration and oxidative stress mitigation. *Mater Today Bio*. 2025;31:101489. doi:10.1016/j.mtbio.2025.101489
5. Ding H, Dai J, Lin J, et al. A 12-month follow-up study of discharged patients with acute pancreatitis: an acute condition with prolonged sequela. *Chinese Med J*. 2024;137(2):250–252. doi:10.1097/CM9.0000000000002847
6. Sohail Z, Shaikh H, Iqbal N, Parkash O. Acute pancreatitis: a narrative review. *J Pak Med Assoc*. 2024;74(5):953–958. doi:10.47391/JPMA.9280
7. Li Y, Yin B, Song Y, et al. A novel ROS-Related chemiluminescent semiconducting polymer nanoplatform for acute pancreatitis early diagnosis and severity assessment. *J Nanobiotechnol*. 2023;21(1):173. doi:10.1186/s12951-023-01937-9
8. Xue M, Lin S, Xie D, et al. The value of CT-based radiomics in predicting the prognosis of acute pancreatitis. *Front Med*. 2023;10:1289295. doi:10.3389/fmed.2023.1289295
9. Diener C, Keller A, Meese E. Emerging concepts of miRNA therapeutics: from cells to clinic. *Trends Genet*. 2022;38(6):613–626. doi:10.1016/j.tig.2022.02.006
10. Luo B, Wang C, Wang Z, Chen C, Peng X, Xu Q. Evaluation of Serum miR-216a, miR-216b, miR-217, miR-92b, miR-375 and miR-148a as potential biomarkers for acute pancreatitis and the role of mir-92b in attenuating caerulein-induced injury and inflammatory responses in AR42J cells. *Comb. Chem. High Throughput Screening*. 2023;26(12):2184–2193. doi:10.2174/1386207326666230202141348
11. Chen YJ, Lin TL, Cai Z, Yan CH, Gou SR, Zhuang YD. Assessment of acute pancreatitis severity via determination of serum levels of hsa-miR-126-5p and IL-6. *Exp Ther Med*. 2021;21(1):26. doi:10.3892/etm.2020.9458
12. Jia A, Yang ZW, Shi JY, Liu JM, Zhang K, Cui YF. MiR-325-3p alleviates acute pancreatitis via targeting RIPK3. *Dig Dis Sci*. 2022;67(9):4471–4483. doi:10.1007/s10620-021-07322-6
13. Ren S, Pan L, Yang L, et al. Interfering hsa_circ_0073748 alleviates caerulein-induced ductal cell injury in acute pancreatitis by inhibiting miR-132-3p/TRAF3/NF-κB pathway. *Cell Cycle*. 2022;21(2):172–186. doi:10.1080/15384101.2021.2014653
14. Huang HYR, Badar S, Said M, et al. The advent of RNA-based therapeutics for metabolic syndrome and associated conditions: a comprehensive review of the literature. *Mol. Biol. Rep*. 2024;51(1):493. doi:10.1007/s11033-024-09457-x
15. Gu Y, Wang G, Ran B. Has_circ_0010220 regulates the miR-574-3p/IL-6 axis to increase doxorubicin resistance in osteosarcoma. *Hum Exp Toxicol*. 2022;41:9603271221131307. doi:10.1177/09603271221131307
16. Chen QY, Jiang YN, Guan X, et al. Aerobic exercise attenuates pressure overload-induced myocardial remodeling and myocardial inflammation via upregulating miR-574-3p in mice. *Circulation*. 2024;17(3):e010569. doi:10.1161/CIRCHEARTFAILURE.123.010569
17. Kang J, Zhang L, Zhang L, Nan N, Liu Y, Hao H. Exosomal miR-574-3p from adipose-derived mesenchymal stem modulates CRIM1/BMPs signaling to restrain chondrocytes hypertrophy and inflammatory response in knee osteoarthritis. *Int Immunopharmacol*. 2025;159:114916. doi:10.1016/j.intimp.2025.114916
18. Yin X, Zhang C. Circulating miR-574-5p shows diagnostic and prognostic significance and regulates oxygen-glucose deprivation (OGD)-induced inflammatory activation of microglia by targeting ATP2B2. *Mol Cell Probes*. 2025;79:102016. doi:10.1016/j.mcp.2025.102016
19. Lv L, Wang X, Shen J, Cao Y, Zhang Q. MiR-574-3p inhibits glucose toxicity-induced pancreatic β-cell dysfunction by suppressing PRMT1. *Diabetol Metab Syndr*. 2022;14(1):99. doi:10.1186/s13098-022-00869-y
20. Banks PA, Bollen TL, Dervenis C, et al. Classification of acute pancreatitis--2012: revision of the Atlanta classification and definitions by international consensus. *Gut*. 2013;62(1):102–111. doi:10.1136/gutjnl-2012-302779
21. Hill M, Tran N. miRNA interplay: mechanisms and consequences in cancer. *Dis Models Mech*. 2021;14(4). doi:10.1242/dmm.047662
22. Mota GAF, Gatto M, Gregolin CS, Souza SLB, Okoshi MP. mRNA, miRNA, lncRNA, ceRNA: the Future of Cardiovascular Research? *Arquivos brasileiros de cardiologia*. 2023;120(4):e20230209. doi:10.36660/abc.20230209
23. Zhang X, Zhu L, Wang X, Xia L, Zhang Y. Advances in the role and mechanism of miRNA in inflammatory pain. *Biomed. Pharmacother*. 2023;161:114463. doi:10.1016/j.biopha.2023.114463
24. Gao J, Chen X, Wei P, Wang Y, Li P, Shao K. Regulation of pyroptosis in cardiovascular pathologies: role of noncoding RNAs. *Mol Ther Nucleic Acids*. 2021;25:220–236. doi:10.1016/j.omtn.2021.05.016
25. Charkiewicz R, Sulewska A, Mroz R, et al. Serum insights: leveraging the power of miRNA profiling as an early diagnostic tool for non-small cell lung cancer. *Cancers*. 2023;15(20):4910. doi:10.3390/cancers15204910
26. Zhao MQ, Cui MY, Jiang QL, Wang JJ, Fan MY, Lu YY. Characterization of duodenal microbiota in patients with acute pancreatitis and healthy controls. *Dig Dis Sci*. 2023;68(8):3341–3353. doi:10.1007/s10620-023-07948-8
27. Han F, Chen H, Chen L, et al. Inhibition of Gasdermin D blocks the formation of NETs and protects acute pancreatitis in mice. *Biochem. Biophys. Res. Commun*. 2023;654:26–33. doi:10.1016/j.bbrc.2023.02.082
28. Lucero D, Wolska A, Aligabi Z, Turecamo S, Remaley AT. Lipoprotein Assessment in the twenty-first Century. *Endocrinol Metab Clinics North Am*. 2022;51(3):459–481. doi:10.1016/j.ecl.2022.02.009
29. Lv JM, Chen JY, Liu ZP, et al. Celluar folding determinants and conformational plasticity of native c-reactive protein. *Front Immunol*. 2020;11:583. doi:10.3389/fimmu.2020.00583
30. Xu XY, Gao Y, Yue CS, et al. Predictive and prognostic potentials of lymphocyte-c-reactive protein ratio upon hospitalization in adult patients with acute pancreatitis. *J Inflamm Res*. 2024;17:1659–1669. doi:10.2147/JIR.S450587
31. Żendzian-Piotrowska M, Ziembicka DM, Łukaszuk B, Kurek K. Impact of acute pancreatic injury on sphingolipid metabolism in the salivary glands. *Biomed Res. Int*. 2020;2020:6403482. doi:10.1155/2020/6403482
32. Li XY, Wang YF, Li N. Circulating microRNA-146a and microRNA-146b exhibit potential to serve as markers for acute pancreatitis management and prognosis. *Eur. Rev. Med. Pharmacol. Sci*. 2020;24(24):12770–12780. doi:10.26355/eurrev_202012_24177
33. Dabrowski A, Boguslowicz C, Dabrowska M, Tribillo I, Gabryelewicz A. Reactive oxygen species activate mitogen-activated protein kinases in pancreatic acinar cells. *Pancreas*. 2000;21(4):376–384. doi:10.1097/00006676-200011000-00008
34. Fu X, Xiu Z, Xu Q, Yue R, Xu H. Interleukin-22 Alleviates Caerulein-Induced Acute Pancreatitis by Activating AKT/mTOR Pathway. *Dig Dis Sci*. 2024;69(5):1691–1700. doi:10.1007/s10620-024-08360-6
35. Ma X, Dong X, Xu Y, et al. Identification of AP-1 as a Critical Regulator of Glutathione Peroxidase 4 (GPX4) Transcriptional Suppression and Acinar Cell Ferroptosis in Acute Pancreatitis. *Antioxidants*. 2022;12(1):100. doi:10.3390/antiox12010100

36. Peng F, Deng X. Ubiquitin-specific protease 7 exacerbates acute pancreatitis progression by enhancing ATF4-mediated autophagy. *Vitro Cell Dev Biol Anim*. 2025;61(3):320–330. doi:10.1007/s11626-024-01009-8
37. Qiu Z, Xu F, Wang Z, et al. Blockade of JAK2 signaling produces immunomodulatory effect to preserve pancreatic homeostasis in severe acute pancreatitis. *Biochem. Biophys. Rep*. 2021;28:101133. doi:10.1016/j.bbrep.2021.101133
38. Zhang Y, Li S, Zhang X, et al. Study on the mechanism of dachaihu decoction in the treatment of acute pancreatitis based on artificial intelligence combined with in vivo experiments. *Comb. Chem. High Throughput Screening*. 2023;26(13):2345–2357. doi:10.2174/1386207326666230202140740
39. Fleming martinez AK, Döppler HR, Bastea LI, et al. Dysfunctional EGFR and oxidative stress-induced PKD1 signaling drive formation of DCLK1+ pancreatic stem cells. *iScience*. 2021;24(1):102019. doi:10.1016/j.isci.2020.102019